Published in final edited form as:
Radiother Oncol. 2011 December ; 101(3): 369–375. doi:10.1016/j.radonc.2011.07.029.

Hypoxia Imaging with [F-18] FMISO-PET in Head and Neck Cancer: Potential for Guiding Intensity Modulated Radiation Therapy in Overcoming Hypoxia-Induced Treatment Resistance

K. R. G. Hendrickson, Ph.D.[a], **M. H. Phillips, Ph.D.**[a], **W. P. Smith, Ph.D.**[b], **L. M. Peterson, B.A.**[c], **K. A. Krohn, Ph.D.**[a,c], and **J. G. Rajendran, M.D.**[a,c]

[a]Department of Radiation Oncology, University of Washington Medical Center, Seattle WA

[b]Department of Radiation Oncology, Stratton VA Medical Center, Albany NY

[c]Department of Radiology, University of Washington Medical Center, Seattle WA

Abstract

Background and Purpose—Positron emission tomography (PET) imaging with [F-18] fluoromisonidazole (FMISO) has been validated as a hypoxic tracer [1, 2]. Head and neck cancer exhibits hypoxia, inducing aggressive biologic traits that impart resistance to treatment. Delivery of modestly higher radiation doses to tumors with stable areas of chronic hypoxia can improve tumor control [3]. Advanced radiation treatment planning (RTP) and delivery techniques such as Intensity Modulated Radiation Therapy (IMRT) can deliver higher doses to a small volume without increasing morbidity. We investigated the utility of co-registered FMISO-PET and CT images to develop clinically feasible RTPs with higher tumor control probabilities (TCP).

Methods—FMISO-PET images were used to determine hypoxic sub-volumes for boost planning. Example plans were generated for ten of the patients in the study who exhibited significant hypoxia. We created an IMRT plan for each patient with a simultaneous integrated boost (SIB) to the hypoxic sub-volumes. We also varied the boost for two patients.

Results—A significant (mean 17%, median 15%) improvement in TCP is predicted when the modest additional boost dose to the hypoxic sub-volume is included.

Conclusions—Combined FMISO-PET imaging and IMRT planning permits delivery of higher doses to hypoxic regions, increasing the predicted TCP (mean 17%) without increasing expected complications.

Keywords

Hypoxia; FDG-PET; IMRT; FMISO-PET

Corresponding author and address for reprints: Joseph G. Rajendran MD, Div of Nuclear Medicine, Box: 356113, University of Washington, Seattle, WA 98195. Phone: (206) 221-4421, rajan@u.washington.edu.

Conflict of Interest Statement

The authors confirm that there are no conflicts of interests, financial or otherwise, in conducting this research with FMISO-PET imaging and radiation therapy planning.

1. Introduction

Head and neck cancer continues to be a significant public health problem in the United States and affects nearly 40,000 persons, causing approximately 10,000 deaths per annum, with greater incidence among veterans. In spite of significant advances in the diagnostic methods for head and neck cancer, many patients still present in late stages with advanced disease, increasing the likelihood for developing hypoxia, a phenomenon shared with other solid tumors [4–8]. One of the hallmarks of tumor hypoxia is the induction of aggressive phenotype that significantly affects the behavior of the hypoxic tumor cells as well as the natural history of cancer in these patients [9]. The cure-limiting effects of hypoxia, particularly radioresistance, have been long known to be a challenging problem to radiobiologists and oncologists. Laboratory experience has documented the need for up to three times as much photon radiation dose to cause the same cytotoxic effect in hypoxic cells as compared to normoxic cells [10], but clinical dose escalation to that level is limited in order to keep normal tissue complication probabilities low [11].

Several methods have been explored to identify, measure, and localize hypoxia in tumors, beginning with clinical assumptions such as tumor grade and size, direct measurements with oxygen electrodes, and indirect methods such as serum biomarkers or immunohistochemistry (IHC) to identify hypoxia-related markers. However, the heterogeneity in regional oxygenation as well as in biological response to hypoxia confounds these tissue-sampling methods. Our goal is to use PET imaging to identify hypoxia, and therefore a more aggressive cancer phenotype, so that specific patients can be selected for more aggressive treatment options. Hypoxia imaging with positron emission tomography (PET) using [F-18] fluoromisonidazole (FMISO) provides a noninvasive method to characterize hypoxia in head and neck cancer [9, 12] and to define hypoxic sub-volumes for dose escalation. A number of previous studies have explored the feasibility of targeting hypoxia and the benefits of dose escalation to hypoxic subvolumes [13, 14].

Radiation treatment techniques such as IMRT [15, 16] are particularly attractive for treating head and neck cancers, where irregular geometry and patient contours in the presence of normal tissues important to quality of life pose unique problems for planning and delivery of effective radiation doses. In addition, the inverse planning methods of IMRT utilizing normal tissue avoidance strategies may permit dose escalation to hypoxic sub-volumes without significantly increasing the risk of complications [17].

In this study, FDG-PET images were used to determine the primary tumor and to identify affected nodes. We used FMISO-PET images to delineate the hypoxic sub-volume for dose escalation and then used IMRT planning techniques to apply different doses to various target sub-volumes and to keep the normal tissue doses within predefined limits. We generated experimental treatment plans for ten patients to explore whether the dose to hypoxic sub-volumes within the gross tumor could be escalated to higher levels while maintaining normal tissue doses within tolerable limits. Our ultimate goal is to improve tumor control and to maintain quality of life.

Currently accepted models were used to estimate tumor control probability (TCP) and normal tissue complication probability (NTCP), including the effect of increased radioresistance of the hypoxic sub-volume [18–21]. Calculations of TCP and NTCP for radiation treatment plans with and without the dose escalation were compared to estimate our ability to control the hypoxic tumor and at the same time limit complications to clinically meaningful levels.

2. Material and methods

2.1 Patients

A total of 102 patients with head and neck squamous cell cancer (HNSCC) were enrolled in a FMISO-PET imaging study of patients with newly diagnosed cancer between April 1994 and August 2007 as part of on-going research protocols. Ten of these patients were randomly selected for inclusion in this subanalysis. These ten patients had an average • 119 weeks of clinical follow up. They were recruited from the University of Washington Medical Center, Harborview Medical Center, and the Veterans Administration Hospital in Seattle. Signed informed consent, as approved by the University of Washington Institutional Review Board and Radiation Safety Committees, was obtained in all cases. Human use of [F-18] FMISO is covered by an Investigational New Drug (IND) authorization and an approval by the institutional Radioactive Drug Research Committee. Only patients with biopsy-proven cancer were included in the study. FMISO and FDG-PET studies were obtained within three days of each other and prior to any therapy. All evaluated patients were systematically staged using direct laryngoscopy and tissue biopsy diagnosis with plain chest radiographs, serum chemistries and liver function panels, and a contrast-enhanced CT scan of the head and neck. American Joint Committee on Cancer (AJCC) version 6 TNM criteria were used for stage delineation. Baseline staging incorporated all physical findings, diagnostic imaging including FDG-PET findings, and available pathology results. Treatment decisions did not take into account FMISO-PET findings, and the actual treatments used for these patients were not altered per the experimental treatment plans. All treatments were performed with curative intent and consisted of standard doses of definitive radiotherapy, chemotherapy, and/or resection, as recommended by a multidisciplinary tumor board. All ten patients in this study were treated with chemoradiation. There is a preponderance of base of tongue (BOT) cancers in this cohort, which is a reflection of the general trend in the patient referrals. Base of tongue cancers provide unique challenges as well as opportunities for treatment planning because of the natural history of spread of cancers arising in the BOT.

2.2 PET Imaging

The PET imaging studies were performed using two scanners: a PET-only Advance scanner [22, 23] and a DSTE PET/CT scanner [24], both manufactured by GE Medical Systems, Waukesha, WI. The PET components of both scanners have similar resolution properties and quantitative accuracies for clinical protocols similar to those used here (data not shown). The axial fields-of-view (FOV) for a single bed position are 15 and 16 cm, respectively, for the two scanners. For all studies the patient data were acquired in 2D mode with corrections applied for attenuation, random and scattered coincidences, detector efficiency variations, deadtime, and a global calibration for converting CPM/voxel to μCi/mL. Images were reconstructed with 2D filtered-backprojection with a reconstructed spatial resolution of approximately 12 mm [22]. For attenuation correction, the PET-only scanner used a transmission scan obtained with rotating Ge-68 rod sources [25], and the PET/CT scanner used a CT-based attenuation correction [26].

FDG Protocol—[F-18] FDG was prepared as described in the literature [27] and was injected intravenously (5 MBq/kg up to ~370 MBq) with patients in a fasting state. Blood sugar levels were determined at the time of imaging for all patients (blood glucose levels <150 mg/dL). Also, all patients were pre-medicated with lorazepam to reduce FDG uptake in skeletal muscle/brown fat. Patient scans started 45 minutes post-injection. Four to five axial fields-of-view (approximately 15 cm each) were obtained that included the base of skull and extended to below the liver. Emission scans were 7 minutes per axial field-of-view.

FMISO Protocol—[F-18] FMISO was prepared as previously described [28]. Patients were not required to fast. Venous access lines were established in each arm, one for FMISO injection and the other for blood sampling. Patients were injected intravenously with 3.7 MBq/kg (0.1 mCi/kg) of [F-18] FMISO, maximum 370 MBq (10 mCi). A single field-of-view emission scan (20 minutes) of the tumor region was obtained. Imaging data were acquired starting approximately 90 – 120 minutes post-injection. These images were reconstructed with the same software corrections and filter size used for FDG. During emission tomography, four venous blood samples were obtained at intervals of 5 minutes. Whole blood samples of 1 mL each were counted in a Cobra multi-channel gamma well counter (Packard Corp., Meriden, CT). Blood activity was averaged and then expressed as μCi/mL decay corrected to time of injection [29].

2.3 Image Registration and Planning for Radiation Treatment

Image preparation for radiation treatment planning utilized the tools of the Pinnacle (Philips Medical Systems, Madison, WI) treatment planning system, including its imbedded Syntegra fusion software (rigid body techniques). Automatic and manual alignment to the treatment planning CT image set used both emission and transmission scans in the case of the PET-only scanner and automatic CT-to-CT alignment in the case of the PET/CT scanner. All registrations were verified by a nuclear medicine physician/radiation oncologist. No estimate of the alignment accuracy was available. The coregistered FDG-PET/CT images, as shown in the example patient in Fig. 1, were used by the physician to guide the manual delineation of gross tumor volumes (GTV) on the treatment planning CT. The FMISO-PET images were used to determine hypoxic sub-volumes (hypoxic GTV) for boost planning. Primary GTVs were expanded by 5 mm to account for microscopic spread (defining the clinical target volume CTV) and set-up uncertainties (defining the planning target volume PTV) but constrained to maintain a 3-mm margin within the skin contours, where appropriate. The FMISO targets were not expanded as the limited PET image resolution already makes the boundaries for the boost target in most cases as large as the corresponding GTV. Additionally, results from Popple *et al*. suggest that it is not necessary to boost the entire hypoxic sub-volume in order to obtain an appreciable increase in tumor control probability [13]. For these reasons we selectively boosted the hypoxic region defined by the FMISO-PET image without adding a margin.

The critical structures of interest included the parotid glands, the spinal cord, and the mandible. Margins of 5 mm were added to the parotid glands and spinal cord to define the planning risk volume (PRV).

Pinnacle radiation treatment planning software, including inverse-planning algorithms, was used to build 7-equiangular-beam IMRT treatment plans using 6-MV photon beams. The simultaneous integrated boost (SIB) IMRT plan prescribed 70 Gy to the primary PTV, 60 Gy to the affected nodes, and a boost of 10 Gy to the hypoxic GTV, to be delivered in 35 fractions. For two of the patients, SIB plans with boost doses of 15 and 20 Gy were also created. Dose volume histogram (DVH) objectives for targets and organs at risk followed the standard of care specifications of our department for head and neck radiation treatment regimes. Target dose limits for critical structures used to guide planning included: spinal cord • 45 Gy, mandible • 70 Gy, and mean dose to parotid glands < 26 Gy with • 40 Gy to 40% of the volume of the ipsilateral parotid gland and • 20 Gy to 20% of the contralateral parotid gland.

2.4 TCP and NTCP Calculations

We calculated the tumor control probability (TCP) using the linear-quadratic (LQ) model [18]. The model used a clinically determined radiation cell kill rate that depends on the

tumor type and biology. Estimates for values of and were derived from clinical studies, with an oxygen enhancement ratio (OER) of 1.5 [30]. We computed the average TCP for 10,000 patients with a Gaussian distribution of values around an average value of 0.47 Gy^{-1} and a width of 0.08 Gy^{-1} with / = 12 Gy, values appropriate for HNSCC [31]. We also included the proliferation effect, where clonogenic tumor cells begin to repopulate some time after radiation treatment begins. The model assumes 35 fractions delivered in 47 days, values consistent with our standard of practice. The lag time for proliferation of 30 days [32] and a tumor-cell doubling time of 3 days [33] were taken from the literature. Of note, because we are comparing treatment regimes that take place over the same time frame, uncertainty in these parameters would affect each regime similarly and would not change the ranking of treatment outcomes [31]. We analyzed both primary targets and treated nodal areas.

Normal tissue complication probabilities (NTCP) were calculated using the Lyman-Kutcher method [19–21], which relies on clinical data to determine the uniform dose that results in a 50% complication rate for an organ ($TD_{50\%}$). Other input parameters describe the volume dependence *n* and slope *m* of the NTCP vs. dose curve. An effective volume approximation was made using a power-law relationship to transform a DVH into a volume at a uniform dose that is assumed to yield the same complication probability as the original histogram [21]. Input values include $TD_{50\%}$ = 66.5 Gy, *n* = 0.05, and *m* = 0.17 for the spinal cord, $TD_{50\%}$ = 46.0 Gy, *n* = 0.70, *m* = 0.18 for the parotid glands, and $TD_{50\%}$ = 72.0 Gy, *n* = 0.07, *m* = 0.10 for the mandible [34–36].

3. Results

Significant hypoxia was identified in all 10 patients in this subanalysis, as shown in Table 1. Data for doses to targets and critical structures in radiotherapy plans with and without the boost dose for the 10 cases included in this report are given in Tables 2 and 3. In all cases the IMRT planning technique permitted the dose escalation without exceeding the clinically acceptable limits for the critical structures. Contralateral parotid glands were spared, except in cases where the primary was central within the head/neck region. Ipsilateral parotid glands were in some cases sacrificed to facilitate target coverage, although in each case this was required even without the dose escalation to the hypoxic sub-volume.

Fig. 2 shows the conformal isodoses around the targets and the sparing of critical structures for Patient ID 6. Fig. 3 presents the DVH for the same patient. Hot spots in the nodes are due to the adjacent or overlapping primary PTV, with its higher dose objective. The hypoxic GTV clearly receives the intended 10-Gy boost. The mean parotid gland doses from the SIB plan are 9.8 Gy on the contralateral gland and 10.1 Gy on the ipsilateral gland.

Table 4 compares the tumor control probability of the primary target and the normal tissue complication probability for each patient plan with and without the boost dose, assuming an OER of 1.5. A significant (mean 17%, median 15%) improvement in TCP is predicted when the modest additional boost dose to the hypoxic sub-volume is included. Insignificant additional gains in TCP of 98.2 and 98.9 for Patient 2 and 98.2 and 98.8 for Patient 9 were found for the 15- and 20-Gy boost plans, respectively. These DVH analyses predict modest increases in TCP while still maintaining clinically acceptable normal tissue doses, as characterized in the NTCP, for the ten patients in this study.

4. Discussion

By inducing resistance to treatment, tumor hypoxia “protects” cancer cells, either as a direct effect (due to lack of molecular oxygen that dampens radiation toxicity) or an indirect effect due to the induction of aggressive phenotypes. Dose escalation to hypoxic sub-volumes with

conventional photon radiation has been investigated in clinical radiation oncology practice to overcome this cure-limiting effect [14, 17, 37, 38]. In current clinical practice, boost treatment (beyond that prescribed to bulky primary tumors and metastatic disease) is guided by CT scans and is based primarily on size criteria. However, it is well established that tumor hypoxia is not related to common clinical parameters including size and histology [5, 39], indicating the need for a more sensitive and specific imaging method to identify and delineate potentially cure-limiting hypoxia in head and neck cancer. Molecular imaging with PET is a more sensitive and specific modality that provides this needed information on the microenvironment [40].

Advantages of FMISO-PET imaging to identify regions of hypoxia include the ready availability of F-18, its easy radiosynthesis, the availability of an IND for FMISO, a simple method for regional quantification based on a static image, and its history of clinical utility. FMISO-PET is becoming a useful tool for clinical applications with several ongoing clinical trials. The 1.5-hour wait following injection has not limited patient compliance and could be considered analogous to the bone scan in this respect. The quantification by comparison of images to a venous blood sample overcomes any limitations of low image contrast. The FMISO images show less contrast compared to that of Cu-ATSM because of its lipophilicity and slower clearance; however, its uptake after 2 hours is a pure reflection of regional pO_2 at the time of radiopharmaceutical administration, providing us with an agent that is overwhelmingly accurate and unequivocally delineates the hypoxic sub-volumes, without any confounding effect of blood flow [9, 12].

After identifying the hypoxic sub-volumes using FMISO-PET imaging, we use the boost GTVs in dose-escalated IMRT plans to explore the feasibility and effect of increased doses to hypoxic sub-volumes. Results from ten patient studies are shown in Tables 2 and 3. In these plans we show that a boost dose of 10 Gy could be accommodated without exceeding normal tissue tolerance doses. In two of the cases, we also explored additional boosts of 15 and 20 Gy.

We estimate the benefit to tumor control and the effect on normal tissue complications using currently accepted models to show an increased TCP of 17% without unacceptable increases in NTCP. The linear quadratic model used to calculate tumor control probability requires an input value for the density of clonogenic stem cells [18]. We assumed a constant density = 1×10^7 cc^{-1} in primary and nodal tumors, although the exact value has not been conclusively determined. Due to these model assumptions, tumor control probability results should not be interpreted as an absolute predictor of tumor control but more as a tool for comparing treatment plans, such as comparing plans without and with the boost dose, as we have done in this study. The value of this analysis is to show improvement in tumor control probability without unacceptable increases in normal tissue complication probability, as shown in Table 4.

In our analysis to estimate tumor control probability and to include the effects of radiation resistance in the hypoxic sub-volume, the cell kill rate in the sub-volume is modified by the OER. Although *in vitro* studies find that for anoxic cells an OER of close to three is appropriate—meaning that anoxic tumor cells are able to survive three times as much radiation as a normal tumor cell—clinical studies with cervical tumors show that an OER = 1.5 is more accurate, perhaps reflecting the fact that some oxygen is present in much of the hypoxic region and/or that the tumor cell population is not homogeneous with respect to pO_2 [30]. This is in contrast with radiobiological experiments *in vitro* where hypoxia is homogeneously present within the cell population studied. For these reasons we used OER=1.5 in our TCP analysis. In our study we used modest boost doses of 10, 15, and 20 Gy. Our analysis of the results of tumor control probability and normal tissue complication

probability provides a convincing case for the benefit of even such a modest boost to select sub-volumes within a tumor.

In clinical practice there is no general agreement on the level of boost dose necessary to overcome the cure-limiting effect of hypoxia, motivating our exploration of the effects of boost doses of 15 and 20 Gy to further evaluate the feasibility of an IMRT-based boost. Additional studies including randomized clinical trials are needed to establish the optimum level of boost to the hypoxic GTV [14, 38].

In our study we employed a SIB within the IMRT plan. Many different strategies for altered fractionation have been utilized clinically to "boost" gross disease, such as accelerated, hyperfractionated, concomitant boost, SIB, and six-days-a-week regimens. They all seem to potentially offer some improvement in locoregional control. SIB is used widely because it is simple to implement (i.e., within a single IMRT plan), it logistically works well with conventional five-days-a-week scheduling, and it represents a modest acceleration to the higher risk volumes, which is well tolerated with concurrent chemotherapy. It is difficult, given the current level of knowledge and clinical experience, to argue which boost delivery strategy would be most effective for addressing hypoxia. However, maintaining the shortest possible treatment time is an important concept to address tumor repopulation. This has been proven in a number of randomized studies and is a strong biological/clinical rationale for SIB vs sequential boosting that protracts treatment time. The SIB strategy has been safely used clinically over the past decade with IMRT [41–45].

We point out that the finding that only two of the ten patients in Table 1 showed local failure indicates the need for additional studies and longer follow-up prior to recommending a change in treatment planning. It should be noted that these were experimental plans and patients received treatment according to established clinical practice. The follow up data in Table 1 does not include treatment with a hypoxic boost. However, our study illustrates the feasibility of an IMRT-based radiation boost to hypoxic sub-volumes and suggests the potential value for achieving better outcomes for this patient population.

On a cautionary note, IMRT is a powerful volume-based inverse-planning modality that can generate tightly conforming isodose contours, but it can still be challenged by patient set-up uncertainties and patient motion [16, 47]. Patient contour deformation and target displacement can further challenge the ability to treat very small sub-volumes such as the identified hypoxic sub-volume. It is likely that image-guided techniques currently under development and in clinical use will be important in obtaining the full benefit of hypoxic-guided boost treatments, especially in head and neck cancers [14, 38].

Another important and currently limiting factor is the dynamic nature of hypoxia and the potential for change in hypoxic volume as treatment progresses. An ideal method should include serial hypoxia imaging beginning pre-therapy and continuing intra-therapy to provide a realistic delineation of the changing hypoxic sub-volume during therapy. Similarly, any hypoxia evaluation method is compounded by the presence of acute versus chronic hypoxia, but the radiobiological principles using boost radiation to overcome treatment resistance are similar for both types of hypoxia. Additional limitations include the influence of genomic and proteomic responses to hypoxia in tissues that promote the increased aggressiveness of clones derived from the hypoxic cells. Thus, while our analysis is focused on local tumor control with a radiation boost, hypoxia has further implications regarding metastatic spread that could adversely affect overall survival and that can be addressed by systemic therapeutic agents.

Furthermore, pre-therapy information on the oxygenation status of a tumor's microenvironment should have additional implications for treatment selection. Presence of

diffuse hypoxia in a tumor might suggest benefit from a systemic approach using a hypoxic cell cytotoxin, e.g. Tirapazamine or a similar compound, or anti-growth factor drugs to combat the limitations of hypoxia [48]. Alternatively, a more focal hypoxia might benefit from a local/regional approach, such as IMRT-based radiation dose escalation to the hypoxic sub-volume [8]. Studies have also established the complementary role of radiation and systemic hypoxia-specific pro-drugs as a synergistic combination in overcoming the hypoxia-induced resistance [12]. We anticipate that FMISO-PET will prove useful for selecting patients for the most appropriate treatment. In this context, its applications include the following as a single modality or as a combination: (1) identification and localization of significant hypoxia; (2) delineation of hypoxic sub-volumes within the GTV for boost radiation; and (3) selection of appropriate systemic agents to complement the boost therapy.

Acknowledgments

We would like to thank Paul Kinahan and all nuclear medicine technologists, radiochemists, and physicists in the division of Nuclear Medicine at the University of Washington Medical Center for their help in PET imaging. We would also like to thank Drs. Upendra Parvathaneni and Jay Liao for their contributions to head and neck planning. This study was supported by NIH grants P01 CA42045 and S10 RR17229.

References

1. Koh WJ, Bergman KS, Rasey JS, et al. Evaluation of oxygenation status during fractionated radiotherapy in human nonsmall cell lung cancers using [F-18]fluoromisonidazole positron emission tomography. Int J Radiat Oncol Biol Phys. 1995; 33:391–398. [PubMed: 7673026]
2. Rajendran JG, Mankoff DA, O'Sullivan F, et al. Hypoxia and glucose metabolism in malignant tumors: evaluation by [18F]fluoromisonidazole and [18F]fluorodeoxyglucose positron emission tomography imaging. Clin Cancer Res. 2004; 10:2245–2252. [PubMed: 15073099]
3. Sovik A, Malinen E, Bruland OS, Bentzen SM, Olsen DR. Optimization of tumour control probability in hypoxic tumours by radiation dose redistribution: a modelling study. Phys Med Biol. 2007; 52:499–513. [PubMed: 17202629]
4. Brizel DM, Sibley GS, Prosnitz LR, Scher RL, Dewhirst MW. Tumor hypoxia adversely affects the prognosis of carcinoma of the head and neck. Int J Radat Oncol Biol Phys. 1997; 38:285–289.
5. Adam M, Gabalski EC, Bloch DA, Ochlert JW, Brown JM, Elsaid AA, Pinto HA, Terris DJ. Tissue oxygen distribution in head and neck cancer patients. Head Neck. 1999; 21:146–153. [PubMed: 10091983]
6. Hockel M, Knoop C, Schlenger K, Vorndran B, Bausmann E, Mitze M, Knapstein PG, Vaupel P. Intra tumoral pO2 predicts survival in advanced cancer of the uterine cervix. Radiother Oncol. 1993; 26:45–50. [PubMed: 8438086]
7. Rasey JS, Koh WJ, Evans ML, et al. Quantifying regional hypoxia in human tumors with positron emission tomography of [18F]fluoromisonidazole: a pretherapy study of 37 patients. Int J Radiat Oncol Biol Phys. 1996; 36:417–428. [PubMed: 8892467]
8. Rajendran JG, Wilson DC, Conrad EU, et al. [(18)F]FMISO and [(18)F]FDG PET imaging in soft tissue sarcomas: correlation of hypoxia, metabolism and VEGF expression. Eur J Nucl Med Mol Imaging. 2003; 30:695–704. [PubMed: 12632200]
9. Rajendran JG, Schwartz DL, O'Sullivan J, et al. Tumor hypoxia imaging with [F-18] fluoromisonidazole positron emission tomography in head and neck cancer. Clin Cancer Res. 2006; 12:5435–5441. [PubMed: 17000677]
10. Evans SM, Koch CJ. Prognostic significance of tumor oxygenation in humans. Cancer Lett. 2003; 195:1–16. [PubMed: 12767506]
11. Wang JZ, Li XA, Mayr NA. Dose escalation to combat hypoxia in prostate cancer: a radiobiological study on clinical data. Br J Radiol. 2006; 79:905–911. [PubMed: 16885177]
12. Rischin D, Hicks RJ, Fisher R, et al. Prognostic significance of [18F]-misonidazole positron emission tomography-detected tumor hypoxia in patients with advanced head and neck cancer randomly assigned to chemoradiation with or without tirapazamine: a substudy of Trans-Tasman Radiation Oncology Group Study 98.02. J Clin Oncol. 2006; 24:2098–2104. [PubMed: 16648512]

13. Popple RA, Ove R, Shen S. Tumor control probability for selective boosting of hypoxic subvolumes, including the effect of reoxygenation. Int J Radiat Oncol Biol Phys. 2002; 54:921–927. [PubMed: 12377346]

14. Rajendran JG, Hendrickson KR, Spence AM, Muzi M, Krohn KA, Mankoff DA. Hypoxia imaging-directed radiation treatment planning. Eur J Nucl Med Mol Imaging. 2006; 33 Suppl 1:44–53. [PubMed: 16763816]

15. Lee N, Puri DR, Blanco AI, Chao KS. Intensity-modulated radiation therapy in head and neck cancers: an update. Head Neck. 2007; 29:387–400. [PubMed: 16358297]

16. Chao KS, Low DA, Perez CA, Purdy JA. Intensity-modulated radiation therapy in head and neck cancers: The Mallinckrodt experience. Int J Cancer. 2000; 90:92–103. [PubMed: 10814959]

17. Thorwarth D, Eschmann SM, Paulsen F, Alber M. Hypoxia dose painting by numbers: a planning study. Int J Radiat Oncol Biol Phys. 2007; 68:291–300. [PubMed: 17448882]

18. Webb S, Nahum AE. A model for calculating tumour control probability in radiotherapy including the effects of inhomogeneous distributions of dose and clonogenic cell density. Phys Med Biol. 1993; 38:653–666. [PubMed: 8346278]

19. Lyman JT. Complication probability as assessed from dose-volume histograms. Radiat Res Suppl. 1985; 8:S13–S19. [PubMed: 3867079]

20. Lyman JT, Wolbarst AB. Optimization of radiation therapy, III: A method of assessing complication probabilities from dose-volume histograms. Int J Radiat Oncol Biol Phys. 1987; 13:103–109. [PubMed: 3804804]

21. Kutcher GJ, Burman C. Calculation of complication probability factors for nonuniform normal tissue irradiation: the effective volume method. Int J Radiat Oncol Biol Phys. 1989; 16:1623–1630. [PubMed: 2722599]

22. Lewellen TK, Kohlmyer S, Miyaoka R, Schubert S, Stearns C. Investigation of the count rate performance of the General Electric Advance Positron Emission Tomograph. IEEE Trans Nucl Sci. 1995; 42:1051–1057.

23. DeGrado TR, Turkington TG, Williams JJ, Stearns CW, Hoffman JM, Coleman RE. Performance Characteristics of a Whole-Body PET Scanner. J Nucl Med. 1994; 35:1398–1406. [PubMed: 8046501]

24. Kinahan P, Vesselle H, Williams J, et al. Performance evaluation of an integrated PET/CT scanner: Discovery STE. J NUCL MED MEETING ABSTRACTS. 2006; 47 392P-a-

25. Daube-Witherspoon M, Carson RE, Green MV. Post-injection transmission attenuation measurements for PET. Nuclear Science, IEEE Transactions on. 1988; 35:757–761.

26. Kinahan PE, Townsend DW, Beyer T, Sashin D. Attenuation correction for a combined 3D PET/CT scanner. Med Phys. 1998; 25:2046–2053. [PubMed: 9800714]

27. Hamacher K, Coenen HH, Stocklin G. Efficient stereospecific synthesis of no-carrier-added 2-[18F]-fluoro-2-deoxy-D-glucose using aminopolyether supported nucleophilic substitution. J Nucl Med. 1986; 27:235–238. [PubMed: 3712040]

28. Adamsen TCH, Grierson JR, Krohn KA. A new synthesis of the labeling precursor for [18F]-fluoromisonidazole. Journal of Labelled Compounds and Radiopharmaceuticals. 2005; 48:923–927.

29. Rajendran J, Muzi M, Peterson LM, Diaz AZ, Spence AM, Schwartz DS, Krohn KA. Analyzing the Results of [F-18] FMISO PET Hypoxia Imaging: What is the best way to Quantify Hypoxia? J Nucl Med. 2002; 43:102.

30. Carlson DJ, Stewart RD, Semenenko VA. Effects of oxygen on intrinsic radiation sensitivity: A test of the relationship between aerobic and hypoxic linearquadratic (LQ) model parameters. Med Phys. 2006; 33:3105–3115. [PubMed: 17022202]

31. Fogliata A, Bolsi A, Cozzi L, Bernier J. Comparative dosimetric evaluation of the simultaneous integrated boost with photon intensity modulation in head and neck cancer patients. Radiother Oncol. 2003; 69:267–275. [PubMed: 14644486]

32. Withers HR, Peters LJ, Taylor JMG, et al. Local control of carcinoma of the tonsil by radiation therapy: An analysis of patterns of fractionation in nine institutions. International Journal of Radiation Oncology*Biology*Physics. 1995; 33:549–562.

33. Maciejewski B, Withers HR, Taylor JM, Hliniak A. Dose fractionation and regeneration in radiotherapy for cancer of the oral cavity and oropharynx: tumor dose-response and repopulation. Int J Radiat Oncol Biol Phys. 1989; 16:831–843. [PubMed: 2921175]
34. Emami B, Lyman J, Brown A, et al. Tolerance of normal tissue to therapeutic irradiation. Int J Radiat Oncol Biol Phys. 1991; 21:109–122. [PubMed: 2032882]
35. Kirkpatrick JP, van der Kogel AJ, Schultheiss TE. Radiation Dose-Volume Effects in the Spinal Cord. International Journal of Radiation Oncology*Biology*Physics. 76:S42–S49.
36. Deasy JO, Moiseenko V, Marks L, Chao KSC, Nam J, Eisbruch A. Radiotherapy Dose-Volume Effects on Salivary Gland Function. International Journal of Radiation Oncology*Biology*Physics. 76:S58–S63.
37. Lee NY, Mechalakos JG, Nehmeh S, et al. Fluorine-18-Labeled Fluoromisonidazole Positron Emission and Computed Tomography-Guided Intensity-Modulated Radiotherapy for Head and Neck Cancer: A Feasibility Study. International Journal of Radiation Oncology*Biology*Physics. 2008; 70:2–13.
38. Chao KS, Bosch WR, Mutic S, et al. A novel approach to overcome hypoxic tumor resistance: Cu-ATSM-guided intensity-modulated radiation therapy. Int J Radiat Oncol Biol Phys. 2001; 49:1171–1182. [PubMed: 11240261]
39. Rajendran JG, Krohn KA. Imaging hypoxia and angiogenesis in tumors. Radiol Clin North Am. 2005; 43:169–187. [PubMed: 15693655]
40. Brahme A. Recent advances in light ion radiation therapy. Int J Radiat Oncol Biol Phys. 2004; 58:603–616. [PubMed: 14751534]
41. Overgaard J, Hansen HS, Specht L, et al. Five compared with six fractions per week of conventional radiotherapy of squamous-cell carcinoma of head and neck: DAHANCA 6&7 randomised controlled trial. The Lancet. 2003; 362:933–940.
42. Fu KK, Pajak TF, Trotti A, et al. A radiation therapy oncology group (RTOG) phase III randomized study to compare hyperfractionation and two variants of accelerated fractionation to standard fractionation radiotherapy for head and neck squamous cell carcinomas: first report of RTOG 9003. International Journal of Radiation Oncology*Biology*Physics. 2000; 48:7–16.
43. Bourhis J, Overgaard J, Audry H, et al. Hyperfractionated or accelerated radiotherapy in head and neck cancer: a meta-analysis. The Lancet. 2006; 368:843–854.
44. Rosenthal DI, Ang KK. Altered radiation therapy fractionation, chemoradiation, and patient selection for the treatment of head and neck squamous carcinoma. Seminars in Radiation Oncology. 2004; 14:153–166. [PubMed: 15095261]
45. Withers HR, Peters LJ. Transmutability of dose and time commentary on the first report of RTOG 90003 (K. K. FU ET AL.). International Journal of Radiation Oncology*Biology*Physics. 2000; 48:1–2.
46. Rajendran JG, Narayanan MV, Hendrickson KRG, et al. 2614: Parametric Images Derived From Kinetic Modeling of Dynamic [F-18] FMISO PET - Evaluating the Feasibility of IMRT Based Dose Escalation to Hypoxic Sub-Volumes. International Journal of Radiation Oncology*Biology*Physics. 2006; 66:S551.
47. Low DA, Chao KS, Mutic S, Gerber RL, Perez CA, Purdy JA. Quality assurance of serial tomotherapy for head and neck patient treatments. Int J Radiat Oncol Biol Phys. 1998; 42:681–692. [PubMed: 9806530]
48. Brown JM. Therapeutic targets in radiotherapy. Int J Radiat Oncol Biol Phys. 2001; 49:319–326. [PubMed: 11173124]

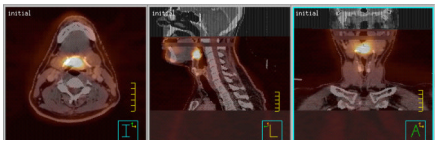

Fig. 1.
Co-registered CT and FMISO-PET images in transaxial, sagittal, and coronal projections for BOT example patient.

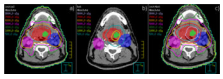

Fig. 2.
Isodose display on axial slices for SIB IMRT plan showing conformal 70-Gy dose around primary PTV (red) and 60-Gy dose around affected nodes (pink and blue). Hypoxic GTV (green) is covered by 80-Gy isodose. Parotid glands (orange and lilac) are avoided by high isodose lines.

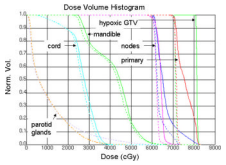

Fig. 3.

Dose volume histogram for plans without (dashed) and with (solid) 10-Gy boost to hypoxic GTV for the sample patient in Figs. 1 and 2.

Table 1

Patient characteristics and tumor parameters determined from FMISO and FDG-PET scans for the study population

Patient ID	Location	Stage[a]	Hypoxic GTV (cc)	FDGSUV	Time to local recurrence
1	Tonsil	T2N3M0	1.0	12.6	31 days
2	Tonsil	T4N2bM0	2.7	3.0[b]	None
3	Tonsil	T4N2M0	5.8	12.1	None
4	BOT	T4N2Mx	6.2	15.3	None
5	BOT	T4N3M0	3.4	10	None
6	BOT	T2N1M0	4.5	14.6	None
7	BOT	T2N2cM0	4.2	9.4	None
8	BOT	T3N2cMx	6.9	10.2	377 days
9	Tonsil	T3N0Mx	1.4	17.6	None
10	Tonsil	T3N3M0	7.4	N/A[c]	None

[a] Staging delineation follows the AJCC version 6 TNM criteria.

[b] FDG scan was taken after start of therapy.

[c] No FDG-PET scan was available for this patient.

Abbreviations: BOT = tumor located in the base of tongue region, SUV = standard uptake value of an FDG image.

Table 2

Dose results for the IMRT plan without the boost dose, where the primary planning target volume (PTV) received a planned dose of 70 Gy

	Without Boost									
Patient	**Primary PTV**		**Ipsi. Parotid Gland**		**Contra. Parotid Gland**		**Spinal Cord**		**Mandible**	
ID	**V100 (%)**	**D95 (Gy)**	**D10 (Gy)**	**Mean (Gy)**	**D10 (Gy)**	**Mean (Gy)**	**D10 (Gy)**	**Mean (Gy)**	**D10 (Gy)**	**Mean (Gy)**
1	96.7	70.2	52.5	32.2	19.2	10.9	30.5	19.3	45.0	22.8
2	98.2	70.7	52.9	19.6	22.4	12.3	29.2	19.0	42.9	25.0
3	95.3	70.0	55.2	31.7	17.1	10.6	30.8	24.4	59.0	36.0
4	98.9	71.0	23.3	13.1	23.3	10.5	28.8	17.4	39.9	27.2
5	94.5	72.9	26.9	10.2	18.6	6.5	30.3	22.3	49.7	35.9
6	97.5	70.6	27.1	10.6	23.5	9.8	32.6	26.0	52.0	40.7
7	97.8	70.6	55.9	19.8	18.4	7.6	32.8	25.2	60.1	46.9
8	97.8	70.6	41.9	16.5	21.4	8.0	28.4	19.5	52.7	33.8
9	97.4	70.7	21.0	15.0	22.6	14.4	30.0	21.3	64.5	34.7
10	95.6	70.1	55.6	31.6	17.8	12.1	32.2	24.9	63.3	37.5
Mean	97.0	70.7	41.2	20.0	20.4	10.3	30.6	21.9	52.9	34.0

Abbreviations: V100 = volume receiving 100% of the planned dose, D*n* = dose received by *n*% of the specified volume.

Table 3

Dose results for the SIB IMRT plans, where the hypoxic sub-volume received a planned dose of 10 Gy

	With 10-Gy Boost									
Patient	**hypoxic GTV**		**Ipsi. Parotid Gland**		**Contra. Parotid Gland**		**Spinal Cord**		**Mandible**	
ID	**V100 (%)**	**D95 (Gy)**	**D10 (Gy)**	**Mean (Gy)**	**D10 (Gy)**	**Mean (Gy)**	**D10 (Gy)**	**Mean (Gy)**	**D10 (Gy)**	**Mean (Gy)**
1	100.0	80.4	57.8	35.8	21.5	12.2	34.1	21.8	50.1	25.2
2	100.0	81.3	53.1	18.8	23.0	11.5	30.1	19.4	45.0	25.0
3	96.7	79.9	59.2	34.0	19.0	11.5	35.1	27.7	66.6	39.9
4	89.4	79.6	25.6	14.3	26.7	12.0	31.6	19.4	43.3	27.6
5	99.6	80.4	29.0	10.9	19.6	6.9	32.4	23.4	54.2	38.7
6	100.0	80.8	26.9	10.1	23.8	9.8	34.1	27.1	52.9	41.9
7	86.2	78.9	56.9	20.1	19.2	7.8	37.1	27.8	67.2	50.7
8	94.5	79.8	42.9	15.5	22.6	8.4	30.1	20.4	59.1	37.0
9	96.7	80.2	22.2	14.3	22.2	14.2	29.9	21.9	64.5	35.4
10	100.0	80.4	64.0	36.7	20.7	14.1	36.5	28.3	72.5	42.0
Mean	96.3	80.2	43.8	21.0	21.8	10.8	33.1	23.7	57.5	36.3

Table 4

Tumor control probability (TCP) predictions and normal tissue complication probability (NTCP) determinations for the 10 patient plans. Top row of NTCP values for each patient corresponds to the initial 70-Gy plan, while the second row corresponds to the plan with the 10-Gy boost.

	TCP			NTCP			
Patient ID	**Initial 70-Gy Plan (%)**	**With 10-Gy Boost (%)**	**Improvement (%)**	**Contra. Parotid Gland (%)**	**Ipsi. Parotid Gland (%)**	**Spinal Cord (%)**	**Mandible (%)**
1	89.9	97.3	8	0.0	6.0	0.1	0.1
				0.0	13.6	0.3	0.1
2	86.5	96.0	11	0.0	0.0	0.0	0.1
				0.0	0.0	0.0	0.1
3	82.4	95.3	16	0.0	5.7	0.0	0.6
				0.0	10.1	0.2	6.1
4	57.2	87.1	52	0.0	0.0	0.0	0.0
				0.0	0.0	0.1	0.1
5	84.1	95.6	14	0.0	0.0	0.0	0.0
				0.0	0.0	0.1	0.0
6	82.6	94.9	15	0.0	0.0	0.1	0.1
				0.0	0.0	0.1	0.8
7	85.5	95.6	12	0.0	0.4	0.1	1.1
				0.0	0.4	0.3	7.2
8	79.9	94.5	18	0.0	0.0	0.0	0.1
				0.0	0.0	0.0	1.0
9	90.4	96.7	7	0.0	0.0	0.0	6.6
				0.0	0.0	0.0	7.0
10	79.3	93.9	18	0.0	6.2	0.1	2.9
				0.0	19.0	0.4	22.8